Contract No:

This document was prepared in conjunction with work accomplished under Contract No. DE-AC09-08SR22470 with the U.S. Department of Energy (DOE) Office of Environmental Management (EM).

Disclaimer:

We put science to work.™

Savannah River National Laboratory™

OPERATED BY SAVANNAH RIVER NUCLEAR SOLUTIONS

A U.S. DEPARTMENT OF ENERGY NATIONAL LABORATORY • SAVANNAH RIVER SITE • AIKEN, SC

2015 In-Situ Gamma-Ray Assay of the West Cell Line in the 235-F Plutonium Fuel Form Facility

A.D. Brand

T.J. Aucott

D.P. DiPrete

February 1, 2016

SRNL-STI-2016-00033 Revision 0

SRNL.DOE.GOV

DISCLAIMER

Printed in the United States of America

Prepared for
U.S. Department of Energy

SRNL-STI-2016-00033
Revision 0

Keywords: 235-F, Non-destructive Assay, Heat-Source Plutonium, PuFF

Retention: *Permanent*

2015 In-Situ Gamma-Ray Assay of the West Cell Line in the 235-F Plutonium Fuel Form Facility

A.D. Brand
T.J. Aucott
D.P. DiPrete

February 1, 2016

Savannah River National Laboratory™
OPERATED BY SAVANNAH RIVER NUCLEAR SOLUTIONS

REVIEWS AND APPROVALS

AUTHORS:

_____
A.D. Brand, Nuclear Measurements Date

_____
T.J. Aucott, Nuclear Measurements Date

_____
D.P. DiPrete, Nuclear Measurements Date

TECHNICAL REVIEW:

_____
R.S. Lee, Nuclear Measurements Date

_____
J.C. Musall, SW&F-Area Engineering Date

APPROVAL:

_____
R.H. Young, Manager Date
Nuclear Measurements

_____
Michael Gilles, Project Manager Date
235-F Risk Reduction

EXECUTIVE SUMMARY

In November and December 2015, scientists from SRNL took a series of in-situ gamma-ray measurements through the windows in front of Cells 6-9 on the west line of the PuFF facility using a shielded, 120% high-purity germanium detector. The detector efficiency was estimated using a combination of MCNP simulations and empirical measurements. Where possible, the distribution of the Pu-238 in the cells was determined using the Germanium Gamma-ray Imager (GeGI). This distribution was then fed into the MCNP model to quantify the Pu-238 in each cell. Data analysis was performed using three gamma rays emitted by Pu-238 (99.85 keV, 152.7 keV, and 766.4 keV) providing three independent estimates of the mass of Pu-238 holdup in each of the cells. The weighted mean of these three results was used as the best estimate of Pu-238 holdup in the West Cell Line of PuFF. The results of the assay measurements are found in the table below along with the results from the assay in 2013 [15] and the scoping assay performed in 2006 [3]. All uncertainties in this table (as well as the rest of the report) are given as 1σ. The total holdup in the West Cell Line was 0.90 ± 0.058 grams. This result is 0.9 g lower than the 2006 estimate and 1.5 g lower than the 2013 estimate. The 2015 assay results were much more precise than the previous assay results. All three assay results agree within a 95% confidence (2 sigma) interval. No further assay work is planned for the West Cell Line prior to clean-up.

Cell	2015 Assay Mass (g)	2013 Assay Mass (g) [15]	2006 Assay Mass (g) [3]
6	0.75 ± 6.3%	2.2 ± 32%	1.78 ± 68%
7	0.15 ± 7.0%	0.25 ± 30%	0.055 ± 82%
8	1.23×10^{-4} ± 12.0%	< 0.004	< 0.00784
9	2.09×10^{-5} ± 24.6%	< 0.004	< 0.00911
Total West Cell Line	0.90 ± 6.4%	2.4 ± 29%	1.8 ± 66%

TABLE OF CONTENTS

LIST OF TABLES

LIST OF FIGURES

LIST OF ABBREVIATIONS

Bq	Becquerel (decays per second)
cm	Centimeter
FWHM	Full-Width at Half-Maximum
GeGI	Germanium Gamma Ray Imager
HEPA	High-Efficiency Particulate Air (filter)
HPGe	High-Purity Germanium Detector
keV	Kilo-Electron-Volt
LaBr	Lanthanum Bromide
LANL	Los Alamos National Laboratory
LN	Liquid nitrogen
MCA	Multi-channel Analyzer
MCNP	Monte-Carlo N-Particle Transport Code
MCNP6	Monte-Carlo N-Particle Transport Code, Version 6
MDA	Minimal Detectable Activity
mm	Millimeter
NDA	Non-destructive Assay
PuFF	Plutonium Fuel Form
PSC	Pajarito Scientific Corporation
SRNL	Savannah River National Laboratory
SRS	Savannah River Site
WBS	Work Breakdown Structure

1.0 Introduction

The Plutonium Fuel Form (PuFF) facility is located in Building 235-F near the geographic center of the Savannah River Site. The facility was used to produce iridium-encapsulated Pu-238 spheres and pellets for use as radioisotope thermal generators, primarily for the space program. The facility is divided between two cell lines, the East Cell Line used to process the powdered Pu-238 oxide raw material into fuel forms and the West Cell Line used to encapsulate the fuel forms in iridium. Between 1978 and 1984, the PuFF facility processed approximately 165 kilograms of Pu-238. In 1984, the facility was placed in "enhanced readiness mode", which consisted of reducing staff to the minimum required to keep the facility maintained in operating condition while waiting for a new mission. During this time, the inert argon atmosphere in the East Cell Line was not maintained. The purpose of the inert argon atmosphere was to prevent corrosion from the high-alpha activity of Pu-238. Corrosion soon made the East Cell Line inoperable, particularly the aluminum remote manipulators. The facility has not been decontaminated since the intent was to continue operations, and after the failure of the manipulators much of the facility is inaccessible [1].

Scoping in-situ gamma-ray assays were performed in the PuFF facility in 2006 [3]. The current estimate of Pu-238 holdup in the facility is based upon these measurements. Using this holdup estimate as a source term, SRS has performed a risk analysis that indicated a seismic event that induces a full-facility fire in 235-F could lead to a 28,800 rem dose to a co-located worker [7]. Based on this risk assessment, SRS is taking steps to decontaminate the facility. One of the first steps taken is to improve upon the quality of the in-situ gamma-ray assay data taken in 2006. The 2006 scoping work consisted of 32 primarily low resolution gamma-ray measurements [3]; the 2013 series of assay measurements included nearly 400 high resolution gamma-ray measurements. These measurements were made in both the East and West Cell Lines with the bulk of the measurements being made on the East Cell Line [15]. This report details the 2015 assays of the West Cell line. Carts and collimators were specially designed to take advantage of the current D&D operations removing the outer cell windows and to actually to hold gamma ray spectrometers inside the cell window cavities to conduct extended count time measurements of the West Cell line cells. The 2015 work consisted of 8 measurements in total. One extended count time measurement (count times ranged from 24 hours to 148 hours) was taken in front of each West Cell Line cell using a 120% efficient high purity germanium (HPGe) detector. This detector was 6 times more efficient than the HPGe detector used in the 2013 assays. The detector was centered on the cell, and was located inside the various cell window cavities, approximately 15 cm from the inner pane of glass. In

addition to the conventional HPGe analysis, Cells 6 and 7 (not enough contamination was present in Cells 8 and 9) were assayed with a GeGI (Germanium Gamma Ray Imager) detector produced by PHDS Co. The GeGI analysis provides a rough map of the distribution of the Pu-238 contamination in the cell analyzed. This detector had two imaging modes: Compton mode, which provides a full response around the detector, and pinhole mode, where the volume visible to the detector could be adjusted to fine tune the response of the system. Cell 6 was assayed using both the Compton mode and the pinhole mode. There was not enough source term in Cell 7 to image using the pin-hole mode. An MCNP model was then built to calibrate/quantify the results of the HPGe measurements. Where possible, the results from the GeGI were used to evaluate several of possible physical distributions for the Pu-238 source term based on the GeGI results. This report describes the West Cell Line hold-up measurements and subsequent data analysis.

This report is in direct support of WBS element 01.29.24.01.09.05 (“Develop Method/Design for Enhanced Characterization, Cells 3-9”) as defined by the Deactivation Project Plan for the 235-F PuFF Facility [11]. Per the Deactivation Project Plan, WBS element 01.29.24.01.09.05 includes "an initial characterization of Cells 6-9 prior to decontamination and material removal activities in those cells." This report documents the final element (exterior measurements coupled with gamma-ray imaging and MCNP modeling) of the enhanced characterization of Cells 6-9 (West Cell Line). This set of measurements completes the characterization of the Pu-238 contamination of the West Cell Line prior to clean-up.

2.0 Data Collection

In November and December 2015, scientists from SRNL took a series of in-situ gamma-ray measurements in front of the windows of Cells 6-9 on the west line of the PuFF facility. The detector used was a 120%-efficient, p-type HPGe detector with a 1.25 mm aluminum endcap. The detector’s efficiency calibration was determined using a Eu-152, Eu-154 and Eu-155 blended source. A Canberra Lynx MCA was used to provide high-voltage and preamp power to the detector as well as process the detector signals. A Panasonic TOUGHBOOK tablet computer was used to run Canberra’s Genie 2000 software [14], which controlled the MCA and saved the spectral data. A specialized cart was fabricated to hold the detector in a horizontal orientation that could be extended into the space available since the removal of the front window. The entire setup consisted of the detector, Sterling cooler, signal cables, Lynx MCA, and tablet computer. Initial data acquisitions were done using tungsten shielding for the sides and back of the HPGe to minimize cross talk and the background. Overnight runs were taken of each cell to ensure enough gamma rays were collected by the system. The major gamma rays (99.85 keV,

152.7 keV, and 766.4 keV) of Pu-238 were clearly present in all acquired spectra except the spectrum taken in front of Cells 8 and 9. The Cell 8 results were quantified from the 99.85 keV and 152.7 keV gamma rays. The Cell 9 results were quantified from the 99.85 keV gamma ray. During all measurements, the face of the detector was located 15 cm from the intact window in each cell. The location of the detector in the plane parallel to the cell floor was recorded for each measurement. A diagram showing the approximate location of each measurement in relation to the West Cell Line geometry is shown in Figure 2-1.

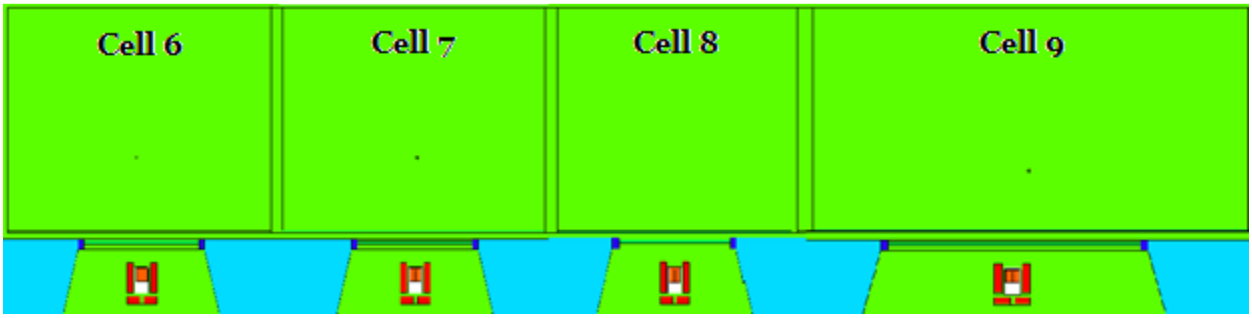

Figure 2-1: West Cell Line Geometry and Assay Locations.

In December 2015, a series of measurements were performed using the GeGI detector to determine the source distribution in the cells. One measurement was taken for Cells 6 and 7 in the large view field Compton mode with 2 additional measurements in the pinhole mode taken in Cell 6 because of the increased mass of Pu-238 in that cell. These measurements each had a view of the entire cell (even though the camera accompanying the GeGI could only capture a picture of roughly half the cell). The GeGI software allowed the scientists to output the data for the full scope of the cell using a mapping feature and those results were overlaid on an overall view of the cell. The GeGI saw a slight bias in Cell 7 (mainly because of the low amounts of Pu-238 present in that cell). However, in Cell 6 the GeGI located a section on the right side of the cell that was more radioactive than its surroundings with respect to the gamma rays emitted from Pu-238. This source distribution was then modeled in MCNP and compared to the previous prediction of Pu-238 hold-up being spread evenly across the cells. All the imaging analyses observed Pu-238 concentrations on the floors; none were observed on the cell walls or HEPAs.

3.0 MCNP Simulations

To estimate the gamma-ray flux at the detector locations per gamma ray emitted by Pu-238, a simulation of the West Cell Line of the PuFF facility was created using the MCNP6 [2] software created by LANL. This program was used to determine the quantity of the Pu-238 hold-up in each cell from the measured efficiency of the detector as well as corrections for attenuation of the gamma-ray flux through intervening material in the cells. All simulations were run until the statistical uncertainty arising from the Monte-Carlo process was negligible.

3.1 Cell Geometry and Materials

Cells 6-9 were modeled as four box-shaped enclosures composed of 316 stainless steel with dimensions based on SRS engineering drawings [5,6]. The walls and ceilings were modeled as 3.2 mm thick and the floor was 4.76 mm thick. The interior dimensions of the cells are given in Table 3-1. There are gaps between adjacent cell walls. The width of the gaps between Cells 6 and 7 as well as Cells 7 and 8 is 11.11 cm. The width of the gap between Cells 8 and 9 is 52.71 cm. The material compositions and densities used in the simulation were taken from Reference 12. These compositions are summarized in Table 3-2.

Each cell contains a cooled storage container, a 55.88-cm diameter, stainless steel cylinder that extends 43.5 cm beneath the cell floor. Each cooled storage container has six interior tubes used to store Pu-238 during production. Rather than include these individual tubes in the MCNP simulation, the wall thickness of the external cylinder was modified as the sum of the actual exterior wall and the wall thickness of interior tubes, the net result being 1.4 cm. The interior of the cooled storage container was modeled as water. Each cell contains a variety of items used to produce, test, and decontaminate the iridium-clad Pu-238 spheres and pellets. The density and thickness of a post-processed steel attenuation layer were adjusted to match the ratios between the 3 photopeaks obtained from the 120% germanium detector system.

Cell	Length (cm)	Width (cm)	Height (cm)
6	201.93	152.4	208.28
7	201.93	152.4	208.28
8	182.88	152.4	208.28
9	274.32	152.4	208.28

Table 3-1: Dimensions of Cells 6-9 used in the MCNP simulation. Length is along the north-south axis, width along the east-west axis.

Material	Density (g/cm^3)	Element	Mass or Atom* Fraction
Stainless Steel 316	7.92**	Silicon	0.010
		Chromium	0.170
		Manganese	0.020
		Iron	0.655
		Nickel	0.120
		Molybdenum	0.025
Carbon Steel	7.82**	Carbon	0.005
		Iron	0.995
Water	1.0	Hydrogen	0.666667*
		Oxygen	0.333333*
Borosilicate Fiberglass	0.02	Boron	0.040063
		Oxygen	0.539561
		Sodium	0.028191
		Aluminum	0.011644
		Silicon	0.377220
		Potassium	0.003321
Germanium	5.323	Germanium	1
Aluminum	2.7	Aluminum	1
Tungsten Shot	9.6	Iron	0.1
		Nickel	0.2
		Tungsten	0.7
Plate Glass	2.5	Oxygen	0.604
		Sodium	0.088
		Silicon	0.252
		Calcium	0.056

Table 3-2: Material Compositions and Densities used in MCNP simulation. Elemental compositions are given by mass fraction except for those indicated by an asterisk (*) that were given by atom fraction. Densities marked with a double asterisk (**) were varied in the geometry to simulate a group of discrete items as a uniform layer of material with a lower density. Elemental compositions were taken from Reference 12.

The location of the detector during each of the measurements of the cells was located at the center of the window from left to right and 7.5 cm above the center horizontal plane of each window. The detector was 15 cm from the window with an angle of the endcap that was parallel to the window. The floor of the cell was 70 cm below the center of the germanium detector. These factors were used in the MCNP model to help account for an attenuation that would occur based on the counting geometry.

3.2 Source Distributions

The photon sources modeled in the MCNP simulation all emitted gamma rays isotropically at three discrete energies, 99.85 keV, 152.7 keV, and 766.4 keV. Two source distributions were modeled to estimate the uncertainty in the overall detector efficiency arising from gamma attenuation and solid angle effects. The source distributions were applied to each cell one at a time. The following source distributions were modeled:

Floor: Photon source uniformly distributed on the floor of the cells (this was used based on the results from the 2013 assay [15])

GeGI: Photon source was adjusted to match the result from the GeGI detector.

3.3 Photon Flux at Detectors

Flux and pulse height light tallies were placed in the MCNP simulation in the germanium crystals of the 120% detector in front of each cell. These tallies give the photon flux per source photon emitted in units of cm^{-2} at the tally location and in the number of pulses that result from the interaction of the Ge crystal and the incoming gamma ray, much like what occurs in the actual system. Since the photopeaks measured by the detector only reflect photons that traveled unscattered from the source distribution to the detector, scattering was turned off in the simulation outside of the crystal (needed for the pulse height tally). Any photons below 99 keV were also removed from transport in the system to save time as well since they would not contribute to the peaks that were being measured (again, except for inside the Ge crystal). This did not remove the effects of attenuation; rather it removes buildup calculations from the simulation, which would only serve to convolute the desired results.

4.0 Data Analysis

To calculate the mass of Pu-238 in each of Cells 6-9 the following formula was used:

$$M_{^{238}Pu} = \frac{N_{net}}{S_{^{238}Pu} \cdot BR_{\gamma} \cdot \varepsilon \cdot t} \qquad \textbf{Equation 4-1}$$

where,

N_{net} = the net count rate for the 120% Germanium detector in front of the cell (or the minimum detectable count rate if applicable),

$S_{^{238}Pu}$ = the specific activity of Pu-238 (6.336×10^{11} Bq/gram ± 0.1%),

BR_{γ} = the absolute branching ratio of the gamma ray used for the analysis,

t = the assay live time,

ε = the detector efficiency at the energy of the gamma ray used for the analysis

4.1 Total Counts

The major three gamma rays emitted by Pu-238 were used for the analysis: 99.85 keV, 152.7 keV, and 766.4 keV. Genie 2000 (a Canberra software product) was used to fit and integrate the three photopeaks in each measured spectrum. Table 4-1 contains the photopeak integrals and uncertainties for each measurement as well as the total counts measured in Cells 6 and 7.

Spectrum Name	99.85 keV Counts	152.7 keV Counts	766.4 keV Counts
Cell 6	$3.65 \times 10^7 \pm 0.02\%$	$9.73 \times 10^6 \pm 0.03\%$	$3.80 \times 10^5 \pm 0.15\%$
Cell 7	$5.81 \times 10^6 \pm 0.04\%$	$1.27 \times 10^6 \pm 0.13\%$	$6.43 \times 10^4 \pm 0.38\%$
Cell 8	$8.34 \times 10^3 \pm 9.43\%$	$3.34 \times 10^3 \pm 18.0\%$	No Peak
Cell 9	$7.91 \times 10^3 \pm 24.3\%$	No Peak	No Peak

Table 4-1: Counts in major Pu-238 photopeaks for each HPGe measurement. There were no photopeaks associated with Pu-238 for some decay energies in the Cell 8 and 9 measurements.

4.2 Detector Efficiency

The detector efficiency for the HPGe was measured using a mixed Europium point source: a mixture of Eu-152, Eu-154, and Eu-155 (EZ-1480-93-9). The europium isotope blend was produced at SRNL from

two liquid standards that were mixed and dried on a planchet. The sources were located 21 cm from the face of the detector directly on its central axis. The efficiency curve for this detector was determined using Canberra's Genie 2000 software [14]. The efficiency curve for the mixed Eu sources is shown in Figure 4-1. The data is shown in Table 4-2.

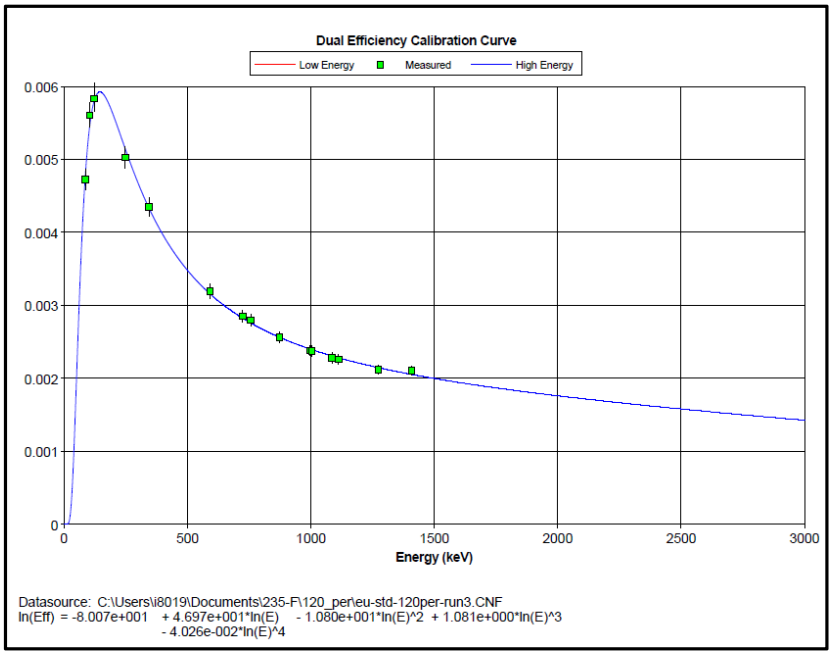

Figure 4-1: Point Source Efficiency for HPGe Detector located 21 cm from Eu-152, Eu-154, and Eu-155 gamma-ray sources.

Energy (keV)	Efficiency	Fit Error (%)	Source Activity Error (%)	Total Error (%)
99.85	4.77×10^{-3}	1.8	3.0	3.5
152.7	5.19×10^{-3}	1.8	3.0	3.5
766.4	2.13×10^{-3}	0.8	3.0	3.1

Table 4-2: Point Source Efficiencies and Associated Uncertainties

4.3 GeGI Operation and Results

The GeGI was placed in front of Cells 6 and 7 and allowed to collect data overnight in Compton imaging mode to determine the location of the Pu-238 in the cell. Cells 8 and 9 did not have enough

contamination to be imaged, so they were not analyzed by the GeGI. The general set-up of the system is shown in Figure 4-2.

Figure 4-2: GeGI set up to move forward to the window of Cell 7 for measurement.

The results from the GeGI in Cell 7 (Figure 4-3) show the general location of the Pu-238 source on the floor for the cell with a slight increase in activity from the center and front right sections. The 2615 keV gamma ray from the impurity Th-228, which has a much higher gamma emission rate than Pu-238, was used to create the image. However, this is a relative scale and the overall number of counts is low enough to where an assumption that the Pu-238 is well spread out over the floor of the cell is valid.

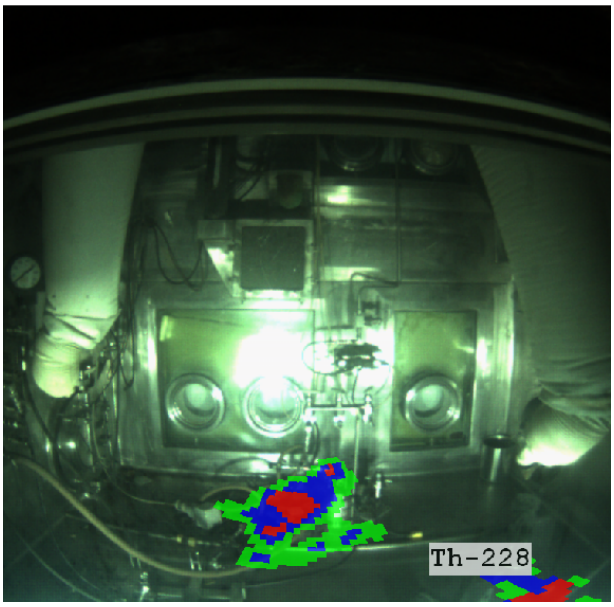

Figure 4-3: Result from Compton image from GeGI in Cell 7.

In Cell 6, the activity was large enough that the result from the GeGI was significant in affecting the distribution of the Pu-238 in the cell as well as the result from the MCNP model. The Compton image, created from the 766 keV gamma ray (Figure 4-4), yielded a source on the right side of the cell about a third of the distance from the window to the back of the cell. This was modeled in MCNP and changed the result of the Cell 6 mass amount by roughly 15% vs a model where the activity was spread evenly across the floor of the cell.

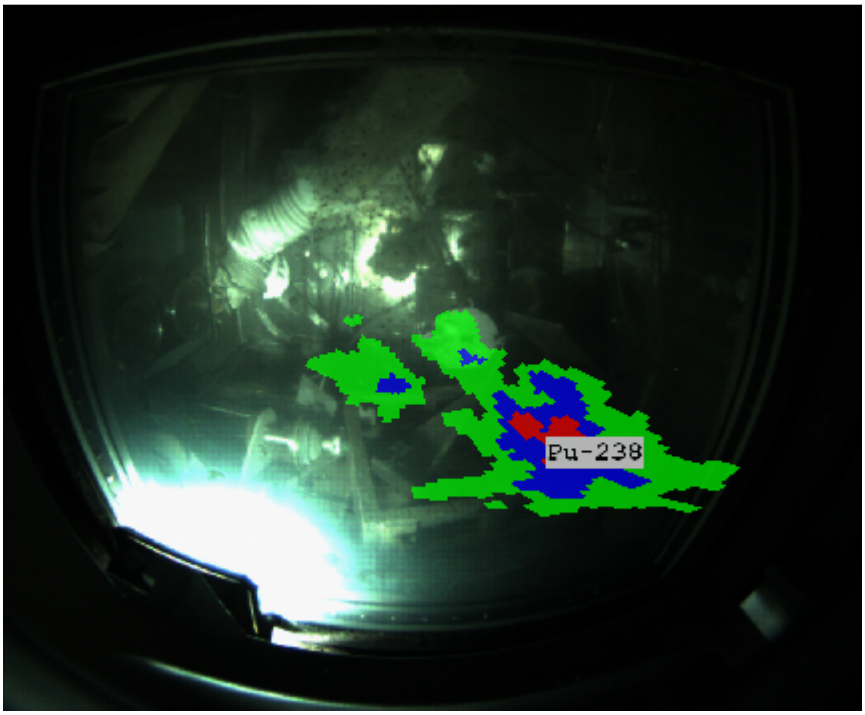

Figure 4-4: Result from Compton image from GeGI in Cell 6.

To fine tune the location and to ensure that it was a localized source, the pinhole imaging mode of the GeGI were then used to confirm the image from the Compton mode (Figure 4-5). A shield was added to the front of the GeGI with a pinhole half a centimeter across in order to generate a pinhole image on the GeGI's sectored HPGe crystal. The highest sensitivity was obtained by imaging the 59 keV gamma ray from Am-241, another impurity in Pu-238. This yielded a figure that confirmed the Compton mode result that a strong source existed in that region a third of the way back from the window to the back wall and on the right side.

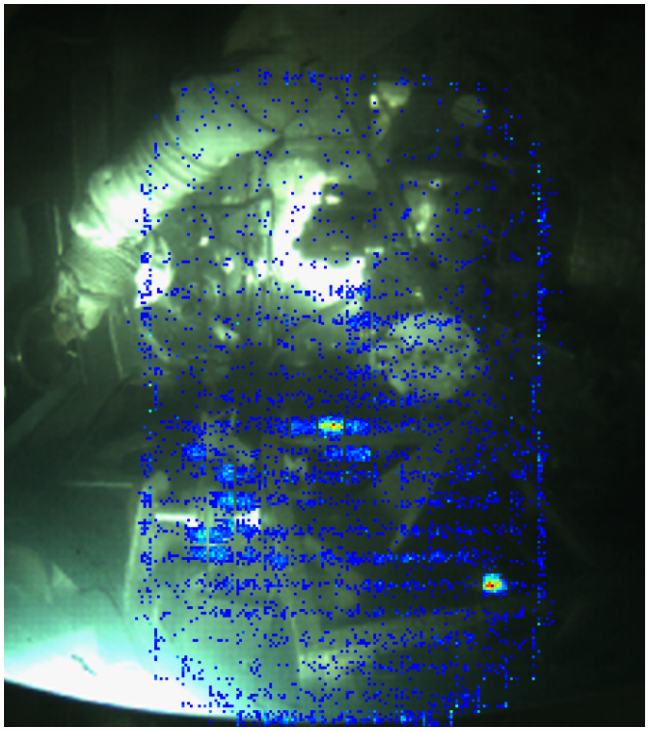

Figure 4-5: Result from Pinhole image from GeGI in Cell 6.

Therefore, the location of the Pu-238 in the MCNP model was adjusted to account for the spatial measurement of the activity seen by the GeGI in Cell 6.

5.0 Assay Results

The assay mass for each cell at each of the three gamma-ray energies used in the analysis was determined using Equation 4-1. The assay masses and parameters used to calculate them for Cells 6-9 may be found in Table 5-1 through Table 5-4, respectively. Since the assay masses from some gamma rays for Cells 8 and 9 were MDAs, no uncertainties were included in parts of Table 5-3 or Table 5-4.

Parameter	99.85 keV Value	152.7 keV Value	766.4 keV Value
Net Count Rate	$3.65 \times 10^{7} \pm 0.02\%$	$9.73 \times 10^{6} \pm 0.03\%$	$3.80 \times 10^{5} \pm 0.15\%$
Point Source Efficiency	$4.77 \times 10^{-3} \pm 3\%$	$5.19 \times 10^{-3} \pm 3\%$	$2.13 \times 10^{-3} \pm 3\%$
MCNP Pulses (#)	$3.05 \times 10^{3} \pm 1.8\%$	$5.13 \times 10^{3} \pm 1.4\%$	$5.77 \times 10^{3} \pm 1.3\%$
Specific Activity (Bq/g)	$6.336 \times 10^{11} \pm 0.1\%$	$6.336 \times 10^{11} \pm 0.1\%$	$6.336 \times 10^{11} \pm 0.1\%$
Branching Ratio	$7.29 \times 10^{-5} \pm 1.1\%$	$9.29 \times 10^{-6} \pm 0.8\%$	$2.20 \times 10^{-7} \pm 9.1\%$
Count Time (s)	83500	83500	83500
Mass (g)	$0.802 \pm 6.8\%$	$0.663 \pm 13.1\%$	$0.811 \pm 8.0\%$

Table 5-1: Assay results for Cell 6 for each of the three gamma-ray energies used in analysis along with the parameters used in the calculation. The specific activity and branching ratios for Pu-238 were taken from the National Nuclear Data Center [13].

Parameter	99.85 keV Value	152.7 keV Value	766.4 keV Value
Net Count Rate	$5.81 \times 10^{6} \pm 0.04\%$	$1.27 \times 10^{6} \pm 0.13\%$	$6.43 \times 10^{4} \pm 0.38\%$
Point Source Efficiency	$4.77 \times 10^{-3} \pm 3\%$	$5.19 \times 10^{-3} \pm 3\%$	$2.13 \times 10^{-3} \pm 3\%$
MCNP Pulses (#)	$3.03 \times 10^{3} \pm 1.8\%$	$5.19 \times 10^{3} \pm 1.4\%$	$5.72 \times 10^{3} \pm 1.3\%$
Specific Activity (Bq/g)	$6.336 \times 10^{11} \pm 0.1\%$	$6.336 \times 10^{11} \pm 0.1\%$	$6.336 \times 10^{11} \pm 0.1\%$
Branching Ratio	$7.29 \times 10^{-5} \pm 1.1\%$	$9.29 \times 10^{-6} \pm 0.8\%$	$2.20 \times 10^{-7} \pm 9.1\%$
Count Time (s)	84600	84600	84600
Mass (g)	$0.164 \pm 11.2\%$	$0.112 \pm 21.3\%$	$0.168 \pm 14.8\%$

Table 5-2: Assay results for Cell 7 for each of the three gamma-ray energies used in analysis along with the parameters used in the calculation. The specific activity and branching ratios for Pu-238 were taken from the National Nuclear Data Center [13].

Parameter	99.85 keV Value	152.7 keV Value	766.4 keV Value
Net Count Rate	$8.34 \times 10^{3} \pm 9.43\%$	$3.34 \times 10^{3} \pm 18.0\%$	No Peak
Point Source Efficiency	$4.77 \times 10^{-3} \pm 3\%$	$5.19 \times 10^{-3} \pm 3\%$	$2.13 \times 10^{-3} \pm 3\%$
MCNP Pulses (#)	$3.17 \times 10^{3} \pm 1.8\%$	$5.57 \times 10^{3} \pm 1.3\%$	$6.15 \times 10^{3} \pm 1.3\%$
Specific Activity (Bq/g)	$6.336 \times 10^{11} \pm 0.1\%$	$6.336 \times 10^{11} \pm 0.1\%$	$6.336 \times 10^{11} \pm 0.1\%$
Branching Ratio	$7.29 \times 10^{-5} \pm 1.1\%$	$9.29 \times 10^{-6} \pm 0.8\%$	$2.20 \times 10^{-7} \pm 9.1\%$
Count Time (s)	83900	83900	83900
Mass (g)	$1.04 \times 10^{-4} \pm 10.1\%$	$1.86 \times 10^{-4} \pm 18.3\%$	$< 2.13 \times 10^{-3}$

Table 5-3: Assay results for Cell 8 for each of the three gamma-ray energies used in analysis along with parameters used in the calculation. The specific activity and branching ratios for Pu-238 were taken from the National Nuclear Data Center [13].

Parameter	99.85 keV Value	152.7 keV Value	766.4 keV Value
Net Count Rate	$7.91 \times 10^{3} \pm 24.3\%$	No Peak	No Peak
Point Source Efficiency	$4.77 \times 10^{-3} \pm 3\%$	$5.19 \times 10^{-3} \pm 3\%$	$2.13 \times 10^{-3} \pm 3\%$
MCNP Pulses (#)	$2.63 \times 10^{3} \pm 2.1\%$	$4.12 \times 10^{3} \pm 1.6\%$	$4.62 \times 10^{3} \pm 1.5\%$
Specific Activity (Bq/g)	$6.336 \times 10^{11} \pm 0.1\%$	$6.336 \times 10^{11} \pm 0.1\%$	$6.336 \times 10^{11} \pm 0.1\%$
Branching Ratio	$7.29 \times 10^{-5} \pm 1.1\%$	$9.29 \times 10^{-6} \pm 0.8\%$	$2.20 \times 10^{-7} \pm 9.1\%$
Count Time (s)	533000	533000	533000
Mass (g)	$2.09 \times 10^{-5} \pm 24.6\%$	$< 8.06 \times 10^{-5}$	$< 1.19 \times 10^{-3}$

Table 5-4: Assay results for Cell 9 for each of the three gamma-ray energies used in analysis along with parameters used in the calculation. The specific activity and branching ratios for Pu-238 were taken from the National Nuclear Data Center [13].

The assay results for each of the three energies considered are essentially completely independent measurements. The final assay result for all cells were based on the most conservative number which was found after adding an amount of steel in the way to account for the attenuation of the three gamma ray energies of interest. This was done to estimate the effect of the stainless steel equipment that was still scattered in the cell. The amount added was determined by minimizing the RMS error between the three peaks relatively to account for this loss in attenuation. This accounted for adding 1.35 g/cm^2 of steel for Cell 6 and 2 g/cm^2 of steel for Cell 7. No steel was added to Cells 8 and 9 because of their low activity levels. The model for Cells 8 and 9 also assumed the activity was spread uniformly across the floors. If the activity was concentrated in a point source in the back corners of the Cells, the activity of that point source would be ~2x the reported activity in Cell 8, and roughly 3x the reported activity of Cell 9.

The final assay masses for Cells 6-9 from the current assay are reported in Table 5-5 along with the previous results from the 2006 and 2013 scoping assays [3,15]. The values reported for Cells 8 and 9 are consistent with the known Pu-238 calibration sources in these cells, each of which accounts for about 0.3 mg of Pu-238. The total Pu-238 holdup measured in the West Cell Line of the PuFF facility for the current assay 0.90 ± 0.058 grams. This result is 0.9 g lower than the 2006 estimate and 1.5 g lower than the 2013 estimate. However, all 3 values for each cell lie within 2 standard deviations of each other which show they agree at a 95% confidence interval.

Cell	2015 Assay Mass (g)	2013 Assay Mass (g) [15]	2006 Assay Mass (g) [3]
6	0.75 ± 6.3%	2.2 ± 32%	1.78 ± 68%
7	0.15 ± 7.0%	0.25 ± 30%	0.055 ± 82%
8	1.23×10^{-4} ± 12.0%	< 0.004	< 0.00784
9	2.09×10^{-5} ± 24.6%	< 0.004	< 0.00911
Total West Cell Line	0.90 ± 6.4%	2.4 ± 29%	1.8 ± 66%

Table 5-5: Final Assay Results for Cells 6-9 compared to 2006 scoping assay results. Uncertainties are reported to 1σ.

6.0 References

[1] "Report of an Investigation into the Deterioration of the Plutonium Fuel Forms Fabrication Facility (PuFF) at the DOE Savannah River Site" Department of Energy – Nuclear Safety, DOE/NS-0002P, (1991)

[2] 6 Monte-Carlo Team. "MCNP – A General N-Particle Transport Code, Version 6, Volume 1: Overview and Theory" Los Alamos National Laboratory. (2013)

[3] D.W. Roberts. "FAMS Hold-Up Measurements for PuFF Process Cells" Savannah River Site. N-CLC-F-00700. (2006)

[4] R.G. Williams III, C.J. Gesh, and R.T. Pagh. "Compendium of Material Composition Data for Radiation Transport Modeling." Pacific Northwest National Laboratory. PNNL-15870, (2006)

[5] "Savannah River Plant Building 235-F Cell Line Plan Cells 6, 7, & 8 Equipment Arrangement Process" Savannah River Site, Drawing W448041, (1974)

[6] "Savannah River Plant Building 235-F Cell Line Plan Cell 9 Equipment Arrangement Process" Savannah River Site, Drawing W448888, (1974)

[7] "Basis for Interim Operation for Building 235-F." Savannah River Site, U-BIO-F-00003 Revision 1, (2013)

[8] J.C. Musall. Private Communication. (2014)

[9] B. Rooney, S. Garner, and P. Felsher. PeakEasy 4.51. Los Alamos National Laboratory. LA-CC-13-040. (2013)

[10] L.A. Currie. "Limits for Qualitative Detection and Quantitative Determination: Application to Radiochemistry." Anal. Chem. 40, 586-593 (1968)

[11] J.K Blankenship and J.C. Musall. "Deactivation Project Plan Plutonium Fuel Form Facility Building 235-F, Metallurgical Building" V-PMP-F00083, Savannah River Site, (2013)

[12] R.J. McConn, Jr., *et al.* "Compendium of Material Composition Data for Radiation Transport Modeling." PIET-43741-TM-963, PNNL-15870 Rev.1, Pacific Northwest National Laboratory, (2011)

[13] E. Brown and J.K Tuli. "Nuclear Data Sheets for A=234." Nuclear Data Sheets 108, 681 (2007)

[14] "Genie 2000 Spectroscopy Software: Operations Manual." Canberra Industries, Inc. (2012)

[15] Couture A.H., DiPrete D.P. "In-Situ Gamma-Ray Assay of the West Cell Line in the 235-F Plutonium Fuel Form Facility" SRNL-STI-2014-00440 (2014).

Appendix A. Example MCNP Input Deck

The input deck for the Material Layer source configuration is given below.

```
ASSAY SIMULATION FOR CELLS 6-9
c
c CCCCCCCCCCCCCCCCCCCCCCCCCCCCCCCCCCCCCCCCCCCCCCCCCCCCCCCCCCCCCCCCCCCCCCCCCCCCCCC
c
c SIMULATION OF CELLS 6-9 WITH Pu-238 GAMMA SOURCES (99, 153, AND
c 766 keV LINES ONLY).  VARIED SOURCE DISTRIBUTIONS AND QUANTITIES OF
c ATTENUATING MATERIALS WILL BE SIMULATED TO ESTIMATE UNCERTAINITY.
c
c GIRDERS BENEATH CELLS ARE SIMULATED AS A UNIFORM LAYER OF CARBON STEEL
c THE DENSITY OF THIS LAYER WAS ESTIMATED USING THE LENGTH OF GIRDER
c MATERIAL FOUND IN EACH CELL FROM DRAWINGS.  THE GIRDER CHANNEL STOCK
c USED WAS NOMINALLY 4.1 LBS/FT.
c
c CELL    GIRDER DENSITY (g/cm^3)
c 6       0.278
c 7       0.318
c 8       0.307
c 9       0.293
c
c COOLED STORAGE UNITS WILL BE SIMULATED BY REMOVING THE INTERIOR STORAGE
c COMPONENTS AND DOUBLING THE THICKNESS OF THE OUTER WALL (TO 1/2 INCH).
c THE COOLERS ARE FILLED WITH WATER
c
c SOURCE IS LOCATED ON THE CELL FLOOR (ONE CELL AT A TIME)
c
c
c CCCCCCCCCCCCCCCCCCCCCCCCCCCCCCCCCCCCCCCCCCCCCCCCCCCCCCCCCCCCCCCCCCCCCCCCCCCCCCC
c
c CELL CARDS
c
c CCCCCCCCCCCCCCCCCCCCCCCCCCCCCCCCCCCCCCCCCCCCCCCCCCCCCCCCCCCCCCCCCCCCCCCCCCCCCCC
c
c CELL 6
c
   10   500 -0.001205 -1 7 60  $ INTERIOR
   11   100   -7.92 -2 1  $ WALLS
   12   200  -0.278 -3  $ GIRDERS
   13   700      -1 -5  $ COOLER INTERIOR
   14   100   -7.92 -4 5  $ COOLER WALLS
   15   500 -0.001205 -6  $ CELL GAP
   16   500 -0.001205 -1 -7  $ MATERIAL LAYER
   17   400    -2.5 -8  $ PLATE GLASS WALL
c
c CELL 7
c
   20   500 -0.001205 -11 17 64  $ INTERIOR
   21   100   -7.92 -12 11  $ WALLS
   22   200  -0.318 -13  $ GIRDERS
```

```
   23   700      -1 -15  $ COOLER INTERIOR
   24   100   -7.92 -14 15  $ COOLER WALLS
   25   500 -0.001205 -16  $ CELL GAP
   26   500 -0.001205 -11 -17  $ MATERIAL LAYER
   27   400    -2.5 -18  $ PLATE GLASS WALL
c
c CELL 8
c
   30   500 -0.001205 -21 27 68  $ INTERIOR
   31   100   -7.92 -22 21  $ WALLS
   32   200  -0.307 -23  $ GIRDERS
   33   700      -1 -25  $ COOLER INTERIOR
   34   100   -7.92 -24 25  $ COOLER WALLS
   35   500 -0.001205 -26  $ CELL GAP
   36   500 -0.001205 -21 -27  $ MATERIAL LAYER
   37   400    -2.5 -28  $ PLATE GLASS WALL
c
c CELL 9
c
   40   500 -0.001205 -31 37 72  $ INTERIOR
   41   100   -7.92 -32 31  $ WALLS
   42   200  -0.293 -33  $ GIRDERS
   43   700      -1 -35  $ COOLER INTERIOR
   44   100   -7.92 -34 35  $ COOLER WALLS
   46   500 -0.001205 -31 -37  $ MATERIAL LAYER
   47   400    -2.5 -38  $ PLATE GLASS WALL
c
c HEPAS
c
   48   500 -0.001205 -61  $ HEPA CUTOUT 6
   49   100   -7.92 -60 61 62  $ HEPA BOX 6
   50   600   -0.02 -62 -63  $ HEPA FILTER 6
   51   500 -0.001205 -62 63  $ HEPA VOID 6
c
   52   500 -0.001205 -65  $ HEPA CUTOUT 7
   53   100   -7.92 -64 65 66  $ HEPA BOX 7
   54   600   -0.02 -66 -63  $ HEPA FILTER 7
   55   500 -0.001205 -66 63  $ HEPA VOID 7
c
   56   500 -0.001205 -69  $ HEPA CUTOUT 8
   57   100   -7.92 -68 69 70  $ HEPA BOX 8
   58   600   -0.02 -70 -63  $ HEPA FILTER 8
   59   500 -0.001205 -70 63  $ HEPA VOID 8
c
   81   500 -0.001205 -73  $ HEPA CUTOUT 9
   82   100   -7.92 -72 73 74  $ HEPA BOX 9
   83   600   -0.02 -74 -63  $ HEPA FILTER 9
   84   500 -0.001205 -74 63  $ HEPA VOID 9
c
c SHIELD WALL
c
   60   300    -2.3 -40 43 44 46 47 49 50 52 53  $ SHIELD WALL
c
   61   500 -0.001205 -43 101 102 103 104 106 $ CELL 6 CUTOUT
   62   500 -0.001205 -46  $ CELL 7 CUTOUT
   63   500 -0.001205 -49 $ CELL 8 CUTOUT
   64   500 -0.001205 -52  $ CELL 9 CUTOUT
```

```
c
   65   100   -7.92 -44 45  $ CELL 6 WINDOW FRAME
   66   100   -7.92 -47 48  $ CELL 7 WINDOW FRAME
   67   100   -7.92 -50 51  $ CELL 8 WINDOW FRAME
   68   100   -7.92 -53 54  $ CELL 9 WINDOW FRAME
c
   69   500 -0.001205 -45 -42  $ CELL 6 WINDOW VOID 1
   70   400    -2.5 -45 42 -41  $ CELL 6 WINDOW
   71   500 -0.001205 -45 41  $ CELL 6 WINDOW VOID 2
c
   72   500 -0.001205 -48 -42  $ CELL 7 WINDOW VOID 1
   73   400    -2.5 -48 42 -41  $ CELL 7 WINDOW
   74   500 -0.001205 -48 41  $ CELL 7 WINDOW VOID 2
c
   75   500 -0.001205 -51 -42  $ CELL 8 WINDOW VOID 1
   76   400    -2.5 -51 42 -41  $ CELL 8 WINDOW
   77   500 -0.001205 -51 41  $ CELL 8 WINDOW VOID 2
c
   78   500 -0.001205 -54 -42  $ CELL 9 WINDOW VOID 1
   79   400    -2.5 -54 42 -41  $ CELL 9 WINDOW
   80   500 -0.001205 -54 41  $ CELL 9 WINDOW VOID 2
c
   88   500 -0.001205 -99 88 4 14 24 34 40 101  $ SURROUNDINGS
   99     0         99  $ THE GRAVEYARD
c DETECTOR SYSTEM
  101   100   -7.92 -101  $ Stainless Steel Plate
  102   800    -9.6 -102  $Left Tungsten Shield
  103   800    -9.6 -103  $Right Tungsten Shield
  104   800    -9.6 -104 105  $Back Tungsten Shield
  105   500 -0.001205 -105  $Gap for cooling pipe
  106   900    -2.7 -106 107  $Outer Al Shell
  107     0         -107 108  $Vacuum
  108   901  -5.323 -108 110  $Dead Layer
  109     0         -109  $Contact Hole
  110   901  -5.323 109 -110  $Active Germanium

c CCCCCCCCCCCCCCCCCCCCCCCCCCCCCCCCCCCCCCCCCCCCCCCCCCCCCCCCCCCCCCCCCCCCC
c
c SURFACE CARDS
c
c CCCCCCCCCCCCCCCCCCCCCCCCCCCCCCCCCCCCCCCCCCCCCCCCCCCCCCCCCCCCCCCCCCCCC
c
c CELL 6
c
    1       rpp 0 201.93 0 152.4 0 208.28  $ INTERIOR
    2       rpp -0.32 202.25 0 152.72 -0.476 208.6  $ EXTERIOR
    3       rpp -0.32 202.25 -1.27 152.72 -8.096 -0.476  $ GIRDERS
    4       rcc 157.16 59.65 -8.096 0 0 -35.72 27.94  $ COOLER EXT
    5       rcc 157.16 59.65 -8.096 0 0 -34.32 26.54  $ COOLER INT
    6       rpp 202.25 213.36 -1.27 152.72 -8.096 208.6  $ CELL GAP
    7        pz 45  $ MATERIAL FILL
    8       rpp -0.32 202.25 -1.27 0 -0.476 208.6  $ PLATE GLASS WALL
c
c CELL 7
c
   11       rpp 213.68 415.61 0 152.4 0 208.28  $ INTERIOR
   12       rpp 213.36 415.93 0 152.72 -0.476 208.6  $ EXTERIOR
```

```
   13       rpp 213.36 415.93 -1.27 152.72 -8.096 -0.476  $ GIRDERS
   14       rcc 261.62 59.65 -8.096 0 0 -35.72 27.94  $ COOLER EXT
   15       rcc 261.62 59.65 -8.096 0 0 -34.32 26.54  $ COOLER INT
   16       rpp 415.93 427.04 -1.27 152.72 -8.096 208.6  $ CELL GAP
   17        pz 30  $ MATERIAL FILL
   18       rpp 213.36 415.93 -1.27 0 -0.476 208.6  $ PLATE GLASS WALL
c
c CELL 8
c
   21       rpp 427.36 610.24 0 152.4 0 208.28  $ INTERIOR
   22       rpp 427.04 610.55 0 152.72 -0.476 208.6  $ EXTERIOR
   23       rpp 427.04 610.55 -1.27 152.72 -8.096 -0.476  $ GIRDERS
   24       rcc 570.87 59.65 -8.096 0 0 -35.72 27.94  $ COOLER EXT
   25       rcc 570.87 59.65 -8.096 0 0 -34.32 26.54  $ COOLER INT
   26       rpp 610.55 663.26 -1.27 152.72 -8.096 208.6  $ CELL GAP
   27        pz 30  $ MATERIAL FILL
   28       rpp 427.04 610.55 -1.27 0 -0.476 208.6  $ PLATE GLASS WALL
c
c CELL 9
c
   31       rpp 663.58 937.9 0 152.4 0 208.28  $ INTERIOR
   32       rpp 663.26 938.21 0 152.72 -0.476 208.6  $ EXTERIOR
   33       rpp 663.26 938.21 -1.27 152.72 -8.096 -0.476  $ GIRDERS
   34       rcc 827.72 59.65 -8.096 0 0 -35.72 27.94  $ COOLER EXT
   35       rcc 827.72 59.65 -8.096 0 0 -34.32 26.54  $ COOLER INT
   37        pz 30  $ MATERIAL FILL
   38       rpp 663.26 938.21 -1.27 0 -0.476 208.6  $ PLATE GLASS WALL
c
c SHIELD WALL
c
   40       rpp -100 1000 -59.06 -5.72 -91.44 213.36  $ WALL
   41        py -7.3  $ GLASS REAR
   42        py -9.21  $ GLASS FRONT
c
   43       arb 163.1 -59.06 123.51 42.01 -59.06 0.95 42.01 $ CUTOUT CELL 6
                -59.06 123.51 163.1 -59.06 0.95 150.97 -12.7 105.89 54.13 -
12.7
                19.53 54.13 -12.7 105.89 150.97 -12.7 19.53 1234 5678 1357
2468
                1458 2367
   44       rpp 54.13 150.97 -12.7 -5.72 19.53 105.89  $ WINDOW FRAME CELL 6
   45       rpp 58.39 146.72 -12.7 -5.72 23.78 101.63  $ WINDOW REGION CELL 6
c
   46       arb 376.14 -59.06 123.51 255.05 -59.06 0.95 255.05 $ CUTOUT CELL
7
                -59.06 123.51 376.14 -59.06 0.95 364.01 -12.7 105.89 267.18
                -12.7 19.53 267.18 -12.7 105.89 364.01 -12.7 19.53 1234 5678
                1357 2468 1458 2367
   47       rpp 267.18 364.01 -12.7 -5.72 19.53 105.89  $ WINDOW FRAME CELL 7
   48       rpp 271.43 359.76 -12.7 -5.72 23.78 101.63  $ WINDOW REGION CELL
7
c
   49       arb 579.66 -59.06 123.51 458.57 -59.06 0.95 458.57 $ CUTOUT CELL
8
                -59.06 123.51 579.66 -59.06 0.95 567.53 -12.7 105.89 470.69
                -12.7 19.53 470.69 -12.7 105.89 567.53 -12.7 19.53 1234 5678
                1357 2468 1458 2367
```

```
   50       rpp 470.69 567.53 -12.7 -5.72 19.53 105.89  $ WINDOW FRAME CELL 8
   51       rpp 474.95 563.28 -12.7 -5.72 23.78 101.63  $ WINDOW REGION CELL
8
c
   52       arb 886.36 -59.06 123.51 694.15 -59.06 0.95 694.15 $ CUTOUT CELL
9
                 -59.06 123.51 886.36 -59.06 0.95 874.24 -12.7 105.89 706.28
                 -12.7 19.53 706.28 -12.7 105.89 874.24 -12.7 19.53 1234 5678
                 1357 2468 1458 2367
   53       rpp 706.28 874.24 -12.7 -5.72 19.53 105.89  $ WINDOW FRAME CELL 9
   54       rpp 710.53 869.98 -12.7 -5.72 23.78 101.63  $ WINDOW REGION CELL
8
c
c HEPAS
c
   60       rpp 67.47 98.9 131.45 152.4 88.58 120.02  $ HEPA BOX 6
   61       rpp 69.85 96.52 131.45 131.76 90.96 117.63  $ HEPA CUTOUT 7
   62       rpp 67.79 98.58 131.76 152.08 88.9 119.7  $ HEPA INTERIOR 6
   63        py 147  $ HEPA REAR
c
   64       rpp 283.69 315.12 131.45 152.4 88.58 120.02  $ HEPA BOX 7
   65       rpp 286.07 312.74 131.45 131.76 90.96 117.63  $ HEPA CUTOUT 7
   66       rpp 284 314.8 131.76 152.08 88.9 119.7  $ HEPA INTERIOR 7
c
   68       rpp 533.56 564.99 131.45 152.4 88.58 120.02  $ HEPA BOX 8
   69       rpp 535.94 562.61 131.45 131.76 90.96 117.63  $ HEPA CUTOUT 8
   70       rpp 533.88 564.67 131.76 152.08 88.9 119.7  $ HEPA INTERIOR 8
c
   72       rpp 745.65 777.08 131.45 152.4 88.58 120.02  $ HEPA BOX 9
   73       rpp 748.03 774.7 131.45 131.76 90.96 117.63  $ HEPA CUTOUT 9
   74       rpp 745.97 776.76 131.76 152.08 88.9 119.7  $ HEPA INTERIOR 9
c
   88       rpp -0.32 938.21 -1.27 152.72 -8.096 208.6  $ ALL CELLS
   99       rpp -110 1100 -100 200 -150 300  $ GRAVEYARD FENCE
c DETECTOR SYSTEM
  101       rpp 75.7 130.3 -71.7 -22.2 58.75 59.7  $ Stainless Steel Plate
  102       rpp 91.5 96.5 -42.5 -22.2 59.7 80  $ Left Tungsten Shield
  103       rpp 109.5 114.5 -42.5 -22.2 59.7 80  $ Right Tungsten Shield
  104       rpp 91.5 114.5 -50.1 -45 59.7 80  $ Back Tungsten Shield
  105       rpp 101.5 104.5 -50.1 -45 59.7 71.1  $ Gap in back shield
  106       rcc 103 -24.7 70 0 -18.3 0 5.4  $Outer Al Shell
  107       rcc 103 -24.85 70 0 -18.15 0 5.25  $Inner Al Shell
  108       rcc 103 -25.35 70 0 -9.44 0 4.36  $Ge Cylinder
  109       rcc 103 -34.79 70 0 8.15 0 0.06  $Contact Hole
  110       rcc 103 -25.5 70 0 -9.29 0 4.21  $Dead/Active Bound

c CCCCCCCCCCCCCCCCCCCCCCCCCCCCCCCCCCCCCCCCCCCCCCCCCCCCCCCCCCCCCCCCCCCC
c
c DATA CARDS
c
c CCCCCCCCCCCCCCCCCCCCCCCCCCCCCCCCCCCCCCCCCCCCCCCCCCCCCCCCCCCCCCCCCCCC
c
mode  p
c
c CCCCCCCCCCCCCCCCCCCCCCCCCCCCCCCCCCCCCCCCCCCCCCCCCCCCCCCCCCCCCCCCCCCC
c
c MATERIAL CARDS
```

```
c
c CCCCCCCCCCCCCCCCCCCCCCCCCCCCCCCCCCCCCCCCCCCCCCCCCCCCCCCCCCCCCCCCCCCC
c
c STAINLESS STEEL 316, DENSITY = 7.92 g/cm^3
c
m100  14000.            -0.01  $ Si
      24000.            -0.17 25000.            -0.02 26000.           -0.655
      28000.            -0.12 42000.           -0.025
c
c CARBON STEEL, DENSITY = 7.82 g/cc
c
m200  6000.            -0.005  $ C
      26000.           -0.995
c
c PORTLAND CEMENT, DENSITY = 2.3 g/cm^3
c
m300  1001.             -0.01  $ H
      6000.            -0.001 8000.         -0.529107 11000.           -0.016
      12000.           -0.002 13000.        -0.033872 14000.        -0.337021
      19000.           -0.013 20000.           -0.044 26000.           -0.014
c
c PLATE GLASS, DENSITY = 2.5 g/cm^3
c
m400  8000.          0.603858  $ O
      11000.         0.088145 14000.         0.251791 20000.         0.056205
c
c AIR, DENSITY = 0.001205 g/cm^3
c
m500  6000.         -0.000124  $ C
      7014.         -0.755268 8016.         -0.231781 18000.        -0.012827
c
c BOROSILICATE FIBERGLASS FILTER, DENSITY = 0.02 g/cm^3
c
m600  5000.         -0.040063  $ B
      8000.         -0.539561 11000.        -0.028191 13000.        -0.011644
      14000.          -0.37722 19000.        -0.003321
c
c WATER, DENSITY = 1.0 g/cm^3
c
m700  1000.          0.666667  $ H
      8000.          0.333333
c
c ALUMINUM, DENSITY = 2.7 g/cm^3
c
m900  13027.               -1
c
c Germanium, Density = 5.323 g/cm^3
c
m901  32000.               -1
c
c TUNGSTEN SHOT, BULK DENSITY = 9.6 g/cc
c
m800  26000.             -0.1  $ Fe
      28000.             -0.2 74000.             -0.7
imp:p   1 68r     0   1 9r            $ 10, 110
nps  1E8     $ NUMBER OF SOURCE PHOTONS
print 10 30 40 50 110 140
```

```
c
c CCCCCCCCCCCCCCCCCCCCCCCCCCCCCCCCCCCCCCCCCCCCCCCCCCCCCCCCCCCCCCCCCCCCCCCCCCC
c
c SOURCE CARDS
c
c CCCCCCCCCCCCCCCCCCCCCCCCCCCCCCCCCCCCCCCCCCCCCCCCCCCCCCCCCCCCCCCCCCCCCCCCCCC
c
c
sdef  PAR=P             $ PHOTON SOURCE
      erg=d1            $ ENERGY GIVEN BY DISTRIBUTION 1
      x=d2              $ SOURCE DISTRIBUTION IN X
      y=d3              $ SOURCE DISTIRBUTION IN Y
      z=0.001           $ SOURCE LOCATED JUST ABOVE FLOOR OF CELLS
c
c ENERGY DISTRIBUTION (DISCRETE LINES)
c
si1 L  0.099853
       0.152720
       0.76639
c
c ENERGY DISTRIBUTION PROBABILITIES (UNNORMALIZED)
c
sp1    1
       1
       1
c
c SOURCE DISTRIBUTION IN X - UNIFORM OVER EXTENT OF CELL 6
c
si2 H 130 140
sp2    0.     1.
c
c SOURCE DISTRIBUTION IN Y - UNIFORM OVER EXTENT OF CELL 6
c
si3 H 45  55
sp3    0.     1.
c
f14:p 110
E14 0 0.098 24i 0.101 0.151 24i 0.154 0.765 24i 0.768
c vol 79j 1
F18:P 110
FC18 PULSE HEIGHT TALLY IN GERMANIUM CRYSTAL
E18     0 1E-5
       0.0499 0.05 0.0599 0.06 0.0699 0.07 0.0799 0.08 0.0899 0.09
       0.0999 0.10 0.1099 0.11 0.1199 0.12 0.1299 0.13 0.1399 0.14
       0.1499 0.15 0.1599 0.16 0.1699 0.17 0.1799 0.18 0.1899 0.19
       0.1999 0.20 0.2999 0.30 0.3999 0.40 0.4999 0.50 0.5999 0.60
       0.6999 0.70 0.7999 0.80 0.8999 0.90 0.9999 1.00 1.2499 1.25
       1.4999 1.50 1.7499 1.75 1.9999 2.00 2.4999 2.50 2.9999 3.00
F28:P 110
FC28 PULSE HEIGHT TALLY IN GERMANIUM CRYSTAL
E28 0 16000i 2
```

Distribution:

A.D. Brand (773-41A)
T.J. Aucott (773-41A)
D.P. DiPrete (773-41A)
R.S. Lee (773-41A)
J.C. Musall (707-7F)
M. L. Gilles (707-7F)
E.T. Sadowski (773-A)
R.H. Young (773-A)
Records Administration (EDWS)